

Studies of the Interactions of H₂ and CO with Pd/SiO₂ Promoted with Li, Na, K, Rb, and Cs

JEFFERY S. RIECK AND ALEXIS T. BELL

Materials and Molecular Research Division, Lawrence Berkeley Laboratory, and Department of Chemical Engineering, University of California, Berkeley, California 94720

Received October 18, 1985; revised March 9, 1986

The interactions of CO and H₂ with Pd/SiO₂ promoted with Li, Na, K, Rb, and Cs have been investigated using temperature-programmed desorption and temperature-programmed surface reaction. Introduction of the promoter following the preparation of the Pd/SiO₂ catalyst causes a small increase ($\approx 7\%$) in the dispersion of the Pd particles. Reduction of the promoted catalysts removes a significant quantity of oxygen from the promoter, but only a small portion of the promoter appears to cover the Pd particles. Alkali promotion of Pd/SiO₂ does not significantly influence the amounts of H₂ and CO that can be adsorbed on the metal. The alkali promoters have a slight influence on the distribution of H₂ adstates but cause a significant change in the distribution of CO adstates. For low reduction temperatures, alkali promotion of Pd/SiO₂ decreases the activity of Pd for the dissociation of CO. However, increasing the reduction temperature increases the CO dissociation activity of the promoted samples due to the increased degree of reduction of the promoter. This enhanced dissociation activity is reversed by the reoxidation of the promoter by the H₂O or CO₂ formed under reaction conditions. The nascent carbon formed by CO dissociation on alkali-promoted Pd/SiO₂ is less reactive than that on unpromoted Pd/SiO₂, and the promoted catalysts have a lower activity for CH₄ synthesis relative to that for unpromoted Pd/SiO₂ decreasing in the order: unpromoted > Li > Na > K > Rb > Cs. © 1986 Academic Press, Inc.

INTRODUCTION

The activity and selectivity of SiO₂- and Al₂O₃-supported Pd catalysts for CO hydrogenation can be altered by promoters. High methanation activity and selectivity is achieved by promoting Pd with titania (1). Promoting Pd with rare earth oxides and MgO increases the specific activity for methanol synthesis (2–4). Alkali promotion of Pd also serves to increase its activity and selectivity for methanol synthesis (5–8). Studies aimed at understanding the effects of transition metal oxide promoters on the catalytic behavior of Pd (1–3, 9–11) have revealed that these effects appear to be due in large measure to the decoration of the supported Pd crystallites by metal oxide moieties derived from the promoter. The alteration in the behavior of Group VIII

metals by alkali promoters has likewise been attributed to the decoration of the crystallites by alkali metal or metal oxide species (12–15). The similarity between these models and that used to explain metal-support interactions (1, 9, 10, 16, 17) suggests that the study of alkali promotion of Pd/SiO₂ may lead to further insights regarding the mechanism for the alteration of the catalytic nature of Pd.

In the present paper we report on experiments aimed at understanding the interactions of H₂ and CO with Pd/SiO₂ promoted with Li, Na, K, Rb, and Cs. The promoters were added to samples taken from a single batch of Pd/SiO₂ to prevent variations in dispersion and in silica composition from influencing the properties of Pd (18–21). The principal techniques used in this study were temperature-programmed desorption

(TPD), temperature-programmed reduction (TPR), and temperature-programmed surface reaction (TPSR).

EXPERIMENTAL

Apparatus. The apparatus used for the present study has been described previously (22–24). The catalysts were placed in a quartz microreactor which could be heated at up to 1 K/s. The desorbing gas was swept from the microreactor by a continuous flow of carrier gas. Analysis of the effluent flow was performed with a quadrupole mass spectrometer. The transfer time from the microreactor to the mass spectrometer was less than 1.5 s. A microprocessor-based data acquisition system was used to direct the mass spectrometer to a series of preselected masses and to record the signal intensity at each mass setting. The catalyst temperature was also recorded by the data acquisition system.

Materials. The methods of catalyst preparation and characterization employed have been described previously (3, 25, 26). The 9% Pd/SiO₂ was obtained by incipient wetness impregnation of Cab-O-Sil HS-5 silica with a solution of H₂PdCl₄ dissolved in 1 N HCl. This catalyst was dried and calcined in a 21% O₂/He mixture at 623 K for 2 h.

The alkali-promoted Pd/SiO₂ catalysts were prepared in a manner similar to that used previously to prepare lanthana-promoted Pd/SiO₂ (3). A portion of the calcined 9% Pd/SiO₂ was impregnated with a solution of the alkali nitrate in deionized H₂O and dried. The catalysts were calcined again and reduced in H₂ at the desired reduction temperature. The loadings of the promoters were chosen so that for the reduced catalysts the ratio of alkali metal atoms to surface Pd atoms would be unity. The promoted and unpromoted catalysts were characterized using H₂-O₂ titration.

Helium and H₂ were purified to remove O₂ and water, and CO was purified to remove metal carbonyls, water, and CO₂. Details of the purification procedures are

given in Ref. (3). The absence of impurities in these gases was established by mass spectrometry.

Experimental procedures. The experimental procedures used in this study are similar to those described in Ref. (3). A mass of catalyst corresponding to 3.8×10^{-6} moles of surface palladium atoms based on H₂-O₂ titration was placed in the microreactor. The mass and the particle size were selected to avoid inter- and intra-particle mass transfer effects (27). The catalysts were reduced for 4 h in H₂ at either 573 or 673 K. Following pretreatment, adsorption was performed by pulsing or flowing the desired gases through the catalyst bed. For temperature-programmed desorption and temperature-programmed surface reaction experiments, flow rates of 50 cm³/min of He and H₂ were used, respectively. The heating rate was 1 K/s for these experiments. The relative activities of the catalysts for CO hydrogenation were determined by ramping the catalyst temperature at 1 K/s in a flow of 75 cm³/min of H₂ and 25 cm³/min of CO. For temperature-programmed reduction experiments, the catalyst was calcined, and then the temperature was ramped at 0.25 K/s in a flow of 200 cm³/min of 1000 ppm H₂ in He. Following each experiment, the mass spectrometer was calibrated against He mixtures containing specified concentrations of H₂ and CO.

The absolute rates of desorption are based on the number of surface Pd atoms present calculated from H₂-O₂ titration. The moles of gas desorbing during an experiment were calculated by first integrating the spectra to find the peak areas, and then multiplying by the proper calibration factor. The initial coverages were found by dividing the number of moles desorbed by the moles of surface Pd present based on H₂-O₂ titration.

RESULTS

H₂-O₂ Titration

The dispersions of the catalysts based on H₂-O₂ titration following reduction at 573

TABLE 1
Pd Dispersion of Pd/SiO₂ and Alkali-Promoted Pd/SiO₂

Catalyst	Dispersion ^a (%)	
	$T_{\text{red}} = 573 \text{ K}$	673 K
9% Pd/SiO ₂	28	28
0.16% Li/(9% Pd/SiO ₂)	35	33
0.54% Na/(9% Pd/SiO ₂)	33	32
0.92% K/(9% Pd/SiO ₂)	33	32
2.0% Rb/(9% Pd/SiO ₂)	32	31
3.1% Cs/(9% Pd/SiO ₂)	34	31

^a Based on H₂-O₂ titration.

and 673 K are given in Table 1. The H₂-O₂ titration results show that the dispersion of the alkali-promoted Pd/SiO₂ catalysts is somewhat higher than that of Pd/SiO₂ following reduction at 573 K. The dispersion of the promoted samples decreases slightly when the reduction temperature is increased to 673 K.

Temperature-Programmed Reduction

TPR experiments were performed to characterize the reducibility of 9% Pd/SiO₂ and the promoted catalysts. The results of the initial TPR experiments, performed on a Pd/SiO₂ sample promoted with RbNO₃, are presented in Fig 1a. During the TPR of this sample, following calcination at 623 K, NO is produced simultaneously with the consumption of H₂. The onset of NO formation during TPR occurs at 425 K. The quantity of NO produced, 3.40×10^{-6} mol, accounts for 89% of the nitrogen present in the catalyst as RbNO₃. These results indicate RbNO₃ undergoes little, if any, decomposition during calcination, but readily decomposes in the presence of H₂. The decomposition of RbNO₃ appears to be catalyzed by the presence of Pd since a sample of 5% RbNO₃/SiO₂ heated in H₂ did not produce NO at temperatures below 500 K. A similar result has been reported by Aika *et al.* (28) who found that Ru promoted the decomposition of CsNO₃.

In light of the preceding results, the procedure for the TPR experiments was altered. Each of the catalysts was calcined at 623 K, reduced in pure H₂ at 573 K, and calcined again at 623 K prior to conducting a second TPR. This procedure enabled the reducibility of the alkali oxide promoter to be observed without interference from precursor decomposition. The spectra for H₂ consumption during TPR are shown in Fig. 1b for the promoted catalysts. The spectrum for the TPR of Pd/SiO₂ consists of a single peak at 343 K with a H₂ consumption of 1.15×10^{-5} mol. The spectra for the Li- and K-promoted samples exhibit two distinct peaks for H₂ consumption at 328 K and 403 K, while the spectra for Rb-, Na-, and Cs-promoted Pd/SiO₂ each consist of a single broad peak near 415 K. The integrated H₂ consumptions for the promoted samples, given in Table 2, are all greater than the uptake by the unpromoted sample.

H₂ and CO TPD

The TPD spectra for H₂ desorption from 9% Pd/SiO₂ and the five promoted catalysts reduced at 573 and 673 K are shown in Figs. 2 and 3, respectively. The initial coverage by adsorbed H atoms, θ_{H}^0 , is based on the amount of H₂ desorbed up to 873 K. For 9% Pd/SiO₂, the saturation coverage is 1.04, independent of the reduction temperature. The saturation coverages for the promoted catalysts reduced at 573 K range between 1.12 and 1.25. Following reduction at 673 K, the saturation coverage decreases to between 0.73 and 0.88.

Figure 2 shows that alkali promotion of Pd/SiO₂ results in subtle changes in the distribution of adstates for H₂ chemisorption. The major peak for H₂ desorption from 9% Pd/SiO₂ is located at 475 K. This peak is accompanied by an unresolved high-temperature shoulder between 550 and 580 K. The shape of the spectrum suggests that another peak is present on the low-temperature side. Figure 2 shows that the major peak for H₂ desorption from the alkali-promoted samples reduced at 573 K is located

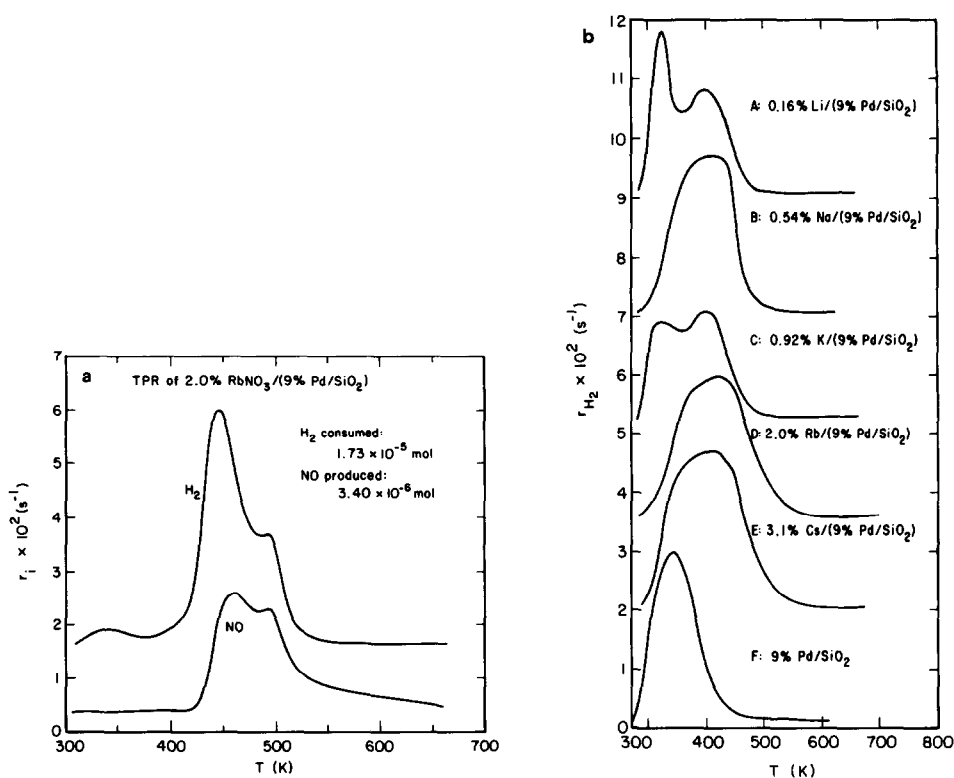


FIG. 1. H_2 consumption during TPR: (a) $RbNO_3$ -promoted Pd/SiO_2 , (b) alkali-promoted Pd/SiO_2 .

at 445–465 K. The high-temperature peak at 550–580 K is much smaller in magnitude. Following promotion with Li and Rb, the low-temperature shoulder is smaller relative to the major peak at 465 K. Increasing the reduction temperature of the promoted samples to 673 K reverses some of the

changes in the TPD spectra. Figure 3 shows that the desorption features for the Na-promoted catalyst reduced at 673 K are quite similar to those of the original Pd/SiO_2 sample. The magnitude of the desorption peak at 550–580 K for the Na-, K-, and Cs-promoted catalysts is not significantly dif-

TABLE 2
 H_2 Uptakes Observed during TPR

Catalyst	H_2 consumption during TPR (mol $\times 10^5$)	Excess H_2 consumption over Pd/SiO_2 ($\times 10^6$ mol)	Oxygen removed per alkali metal atom (mol/mol)
9.0% Pd/SiO_2	1.15	—	—
0.16% Li/(9% Pd/SiO_2)	1.71	6.2	1.61
0.54% Na/(9% Pd/SiO_2)	1.52	3.7	0.96
0.92% K/(9% Pd/SiO_2)	1.57	4.2	1.10
2.0% Rb/(9% Pd/SiO_2)	1.40	2.1	0.55
3.1% Cs/(9% Pd/SiO_2)	1.47	3.5	0.92

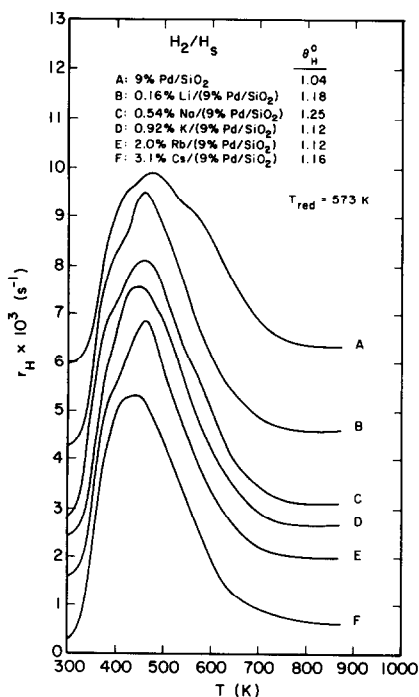


FIG. 2. Effects of alkali promotion on the H₂ TPD spectra for 9% Pd/SiO₂; $T_{\text{red}} = 573$ K.

ferent from that for Pd/SiO₂. However, the magnitude of the high-temperature peak remains diminished for the Rb- and Li-promoted samples. The low-temperature shoulder is more prominent for all the promoted samples relative to unpromoted Pd/SiO₂. Thus, alkali promotion of Pd/SiO₂ results in changes in the distribution of adstates with only a modest suppression in chemisorption capacity.

The CO desorption spectra for 9% Pd/SiO₂ and the five alkali-promoted samples reduced at 573 and 673 K are shown in Figs. 4a and 5a, respectively. The associated spectra for the CO₂ evolved during CO desorption are given in Figs. 4b and 5b. Since no H₂ was observed during the CO TPD experiments, the water-gas shift reaction can be ruled out as a possible source of CO₂. Therefore, the CO₂ formed can be attributed totally to the disproportionation of CO: $2 \text{ CO}_{\text{ads}} \rightarrow \text{C}_{\text{ads}} + \text{CO}_2$. The initial coverage of CO, θ_{CO}^0 , given in Figs. 4a and

5a is taken to be the amount of CO desorbed, θ_{CO} , plus twice the amount of CO₂ produced. The equivalent coverage of CO converted to CO₂ is given by θ_{CO_2} .

The spectrum for CO TPD from 9% Pd/SiO₂ shown in Fig. 4a consists of four peaks located at 410, 530, 650, and 790 K. The saturation coverage is 0.88. The saturation coverages of the promoted catalysts reduced at 573 K, given in Fig. 4a, range between 0.92 and 1.12. These uptakes are slightly less than those measured for H₂. Comparison of the spectra in Fig. 4a for the promoted and unpromoted samples reveals that alkali promotion causes a redistribution of the CO adstates. An increase in the rates of CO desorption is observed for temperatures below 573 K along with a decrease at higher temperatures for all of the promoted samples. Moreover, for the K- and Rb-promoted Pd/SiO₂, the peak at 410 K now appears as two peaks at 370 and 440 K.

Figure 4b shows that all six catalyst pro-

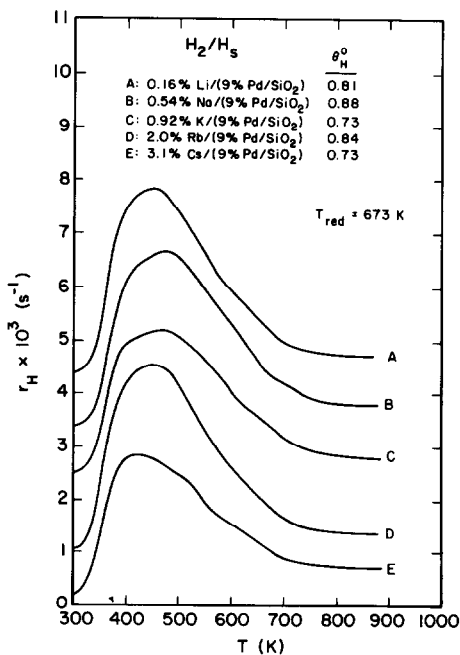


FIG. 3. Effects of alkali promotion on the H₂ TPD spectra for 9% Pd/SiO₂; $T_{\text{red}} = 673$ K.

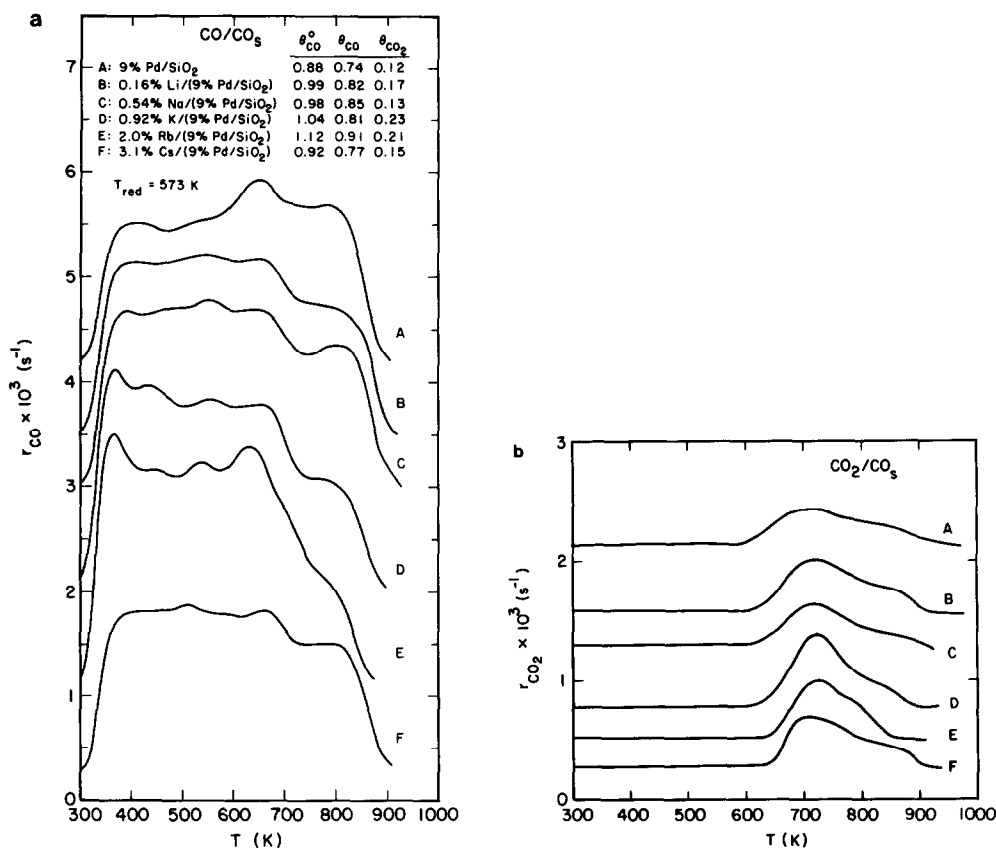


FIG. 4. Effects of alkali promotion on the desorption products observed during CO TPD from 9% Pd/SiO₂: (a) CO, (b) CO₂; $T_{red} = 573 \text{ K}$.

duce significant amounts of CO₂ during CO TPD following reduction at 573 K. CO₂ formation is observed over 9% Pd/SiO₂ at temperatures above 580 K and reaches a maximum rate at 720 K. The onset of CO₂ formation over the promoted catalysts occurs at slightly higher temperatures, between 600 and 630 K, but the peak locations for maximum CO₂ production are not significantly different from that for unpromoted Pd/SiO₂.

Reduction of unpromoted Pd/SiO₂ at 673 K had no effect on the TPD spectrum or θ_{CO}^0 ; both were identical to those seen in Fig. 4a. Figure 5a shows, however, that reduction of the promoted samples at 673 K does cause a small decrease in the initial coverage of CO, an effect similar to that observed for H₂. Comparison of the CO

spectra presented in Figs. 4a and 5a shows that the higher reduction temperature suppresses the desorption of CO at temperatures below 573 K and increases the desorption of CO at temperatures above 723 K. The rate of desorption in the range of 573 to 723 K decreases when the promoted samples are reduced at 673 K, relative to what is observed for reduction at 573 K.

The spectra in Fig. 5b show that the onset of CO₂ formation shifts to lower temperatures when the promoted catalysts are reduced at 673 K rather than 573 K, and, in fact, the threshold temperatures in this case are all lower than that for unpromoted Pd/SiO₂. It is noted, however, that θ_{CO_2} and the maximum rate of CO₂ formation are both lower when reduction is carried out at 673 K.

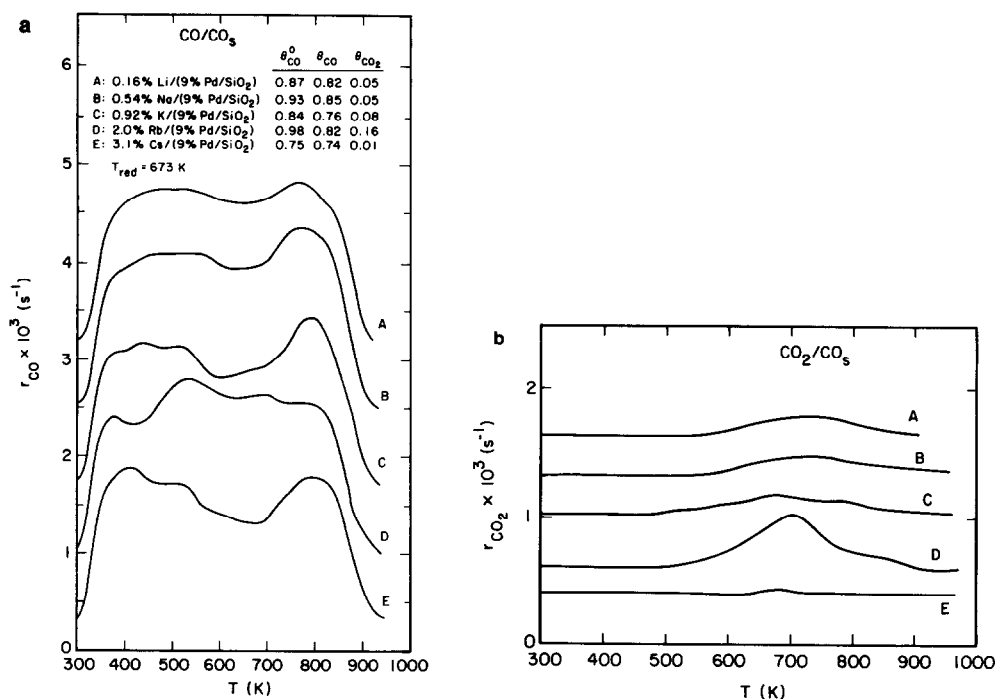


FIG. 5. Effects of alkali promotion on the desorption products observed during CO TPD from 9% Pd/SiO₂: (a) CO, (b) CO₂; $T_{red} = 673$ K.

TPSR of H₂ and CO

TPSR experiments were performed on the promoted catalysts to gain further information regarding the influence of the alkali promoters on catalyst performance. The methane features for the TPSR of CO following adsorption at room temperature are given in Figs. 6a and 7a for 9% Pd/SiO₂ and the five promoted catalysts reduced at 573 and 673 K, respectively. The spectra for CO desorption during the TPSR are given in Figs. 6b and 7b. The initial coverages by CO, θ_{CO}^0 , are in good agreement with those shown in Figs. 4a and 5a for CO TPD. The methane spectrum for 9% Pd/SiO₂ exhibits a single peak at 625 K. For the samples reduced at 573 K, alkali promotion results in a slight upscale shift in the peak temperature for methane production. The peak locations increase in the order: unpromoted (625 K) < Li (630 K) = Na (630 K) = K (630 K) < Rb (640 K) < Cs (645 K). The

fraction of initially adsorbed CO which reacts to give CH₄, $X_{CH_4/CO}$, is between 0.45 and 0.51 for all six catalysts. Following reduction at 673 K, the peak locations increase in the same order: Pd/SiO₂ (625 K) < Li (630 K) = Na (630 K) < K (633 K) < Rb (640 K) < Cs (650 K). The range of $X_{CH_4/CO}$ is between 0.32 and 0.42 for the promoted samples. Thus, alkali promotion makes Pd/SiO₂ less active for methanation.

The effects of alkali promotion on the activity of Pd/SiO₂ for CO dissociation were investigated by performing the TPSR experiments following CO adsorption at elevated temperatures. Figure 8 shows the CH₄ produced by Pd/SiO₂ and the promoted catalysts reduced at 573 K during the TPSR of CO adsorbed for 5 min at 573 K. For 9% Pd/SiO₂, a low-temperature peak is observed at 478 K along with a peak at 630 K. This low-temperature peak is attributed to the hydrogenation of surface carbon deposited during the adsorption step (3). The ini-

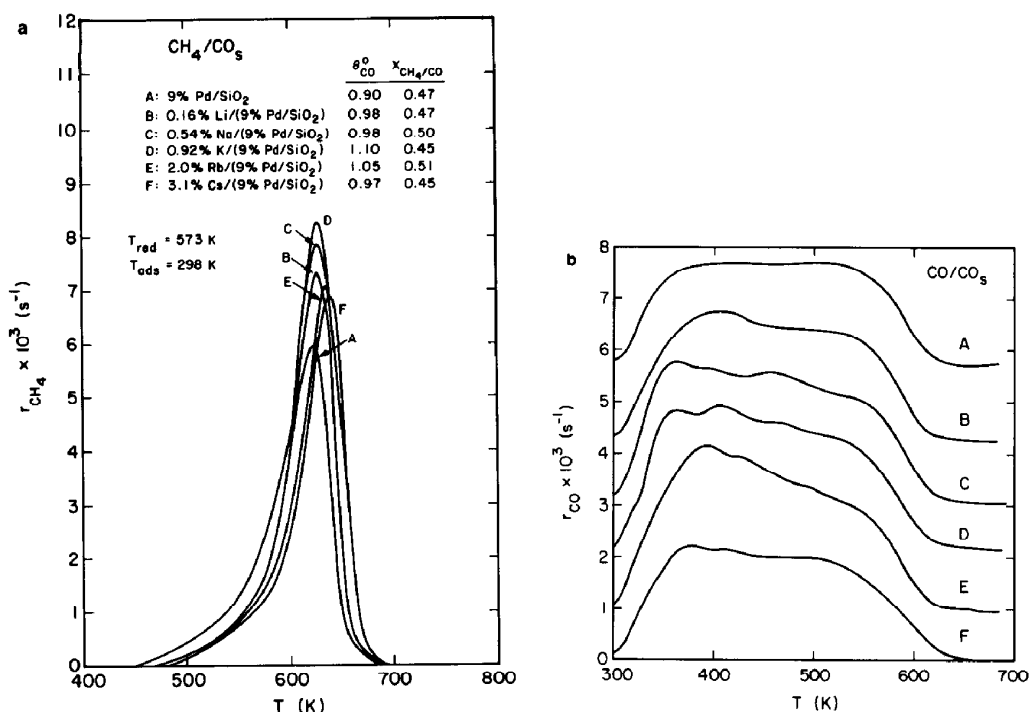


FIG. 6. Effects of alkali promotion on the products formed during TPSR of CO adsorbed on 9% Pd/SiO₂: (a) CH₄, (b) CO; $T_{\text{red}} = 573 \text{ K}$.

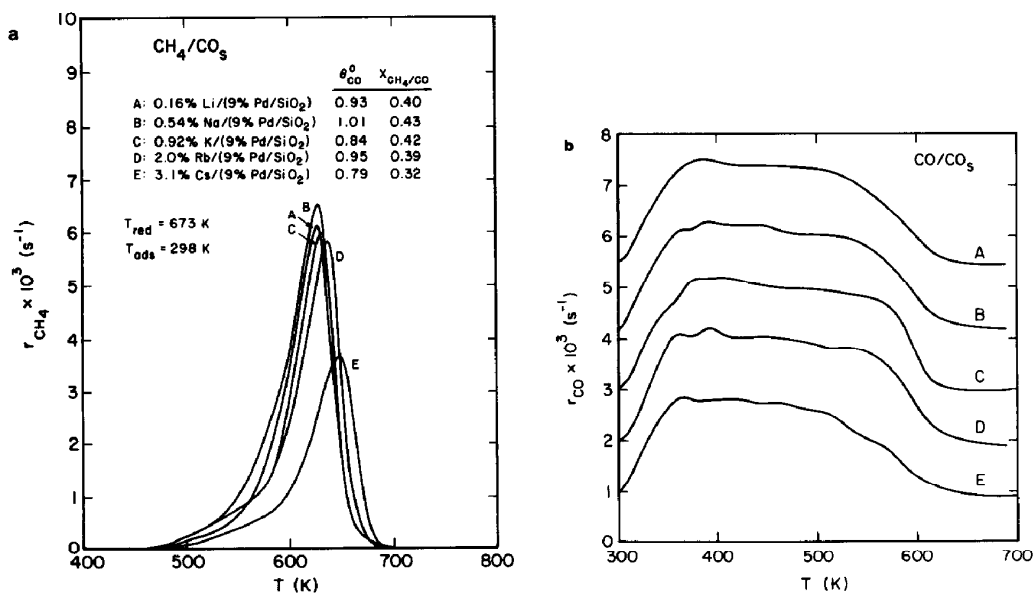


FIG. 7. Effects of alkali promotion on the products formed during TPSR of CO adsorbed on 9% Pd/SiO₂: (a) CH₄, (b) CO; $T_{\text{red}} = 673 \text{ K}$.

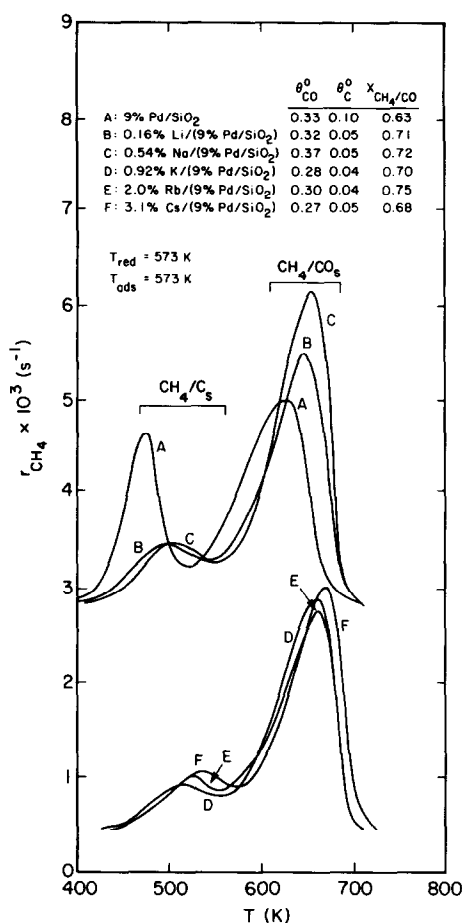


FIG. 8. Effects of CO adsorption temperature on CH₄ formation during TPSR of CO adsorbed on alkali-promoted Pd/SiO₂; $T_{red} = 573\text{ K}$, $T_{ads} = 573\text{ K}$.

tial coverage by adsorbed carbon, as determined from the quantity of CH₄ produced in the low-temperature peak, is given by θ_C^0 . For adsorption at 573 K, 0.10 of a monolayer of surface carbon is deposited on Pd/SiO₂. The spectra in Fig. 8 reveal that the promoted catalysts exhibit much smaller peaks due to the methanation of surface carbon. Thus, the promotion of Pd/SiO₂ with an alkali lowers its activity for CO dissociation following reduction at 573 K.

Figure 8 also reveals that the carbon deposited on the promoted samples during CO dissociation is less reactive with H₂ than that on unpromoted Pd/SiO₂, as

shown by the higher peak temperatures for the low-temperature CH₄ peak. Thus, it is seen from the peak locations that the reactivity of the surface carbon decreases in the order: unpromoted (478 K) > Li (498 K) > Na (508 K) > K (520 K) > Rb (530 K) > Cs (535 K).

Figure 9 shows the CH₄ spectra obtained during the TPSR of CO adsorbed for 5 min at 573 K for the five promoted catalysts reduced at 673 K. For this reduction temperature, more carbon was deposited on each of the promoted samples than on Pd/SiO₂. The amount of carbon deposited increases in the order: unpromoted < Rb < K < Na < Li < Cs. Thus, Fig. 9 shows that the reduction temperature can influence the activity of the promoted samples for CO dissociation. However, comparison of Figs. 8 and 9 reveals that the peak locations for the hydrogenation of surface carbon do not vary with reduction temperature.

The influence of H₂ on the dissociation of CO was investigated by adsorbing CO at 573 K in the presence of 10% H₂ following reduction at 573 K. Figure 10 shows the

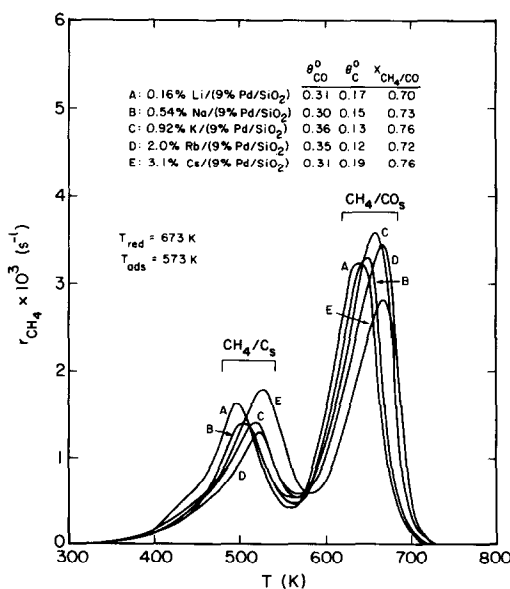


FIG. 9. Effects of CO adsorption temperature on CH₄ formation during TPSR of CO adsorbed on alkali-promoted Pd/SiO₂; $T_{red} = 673\text{ K}$, $T_{ads} = 573\text{ K}$.

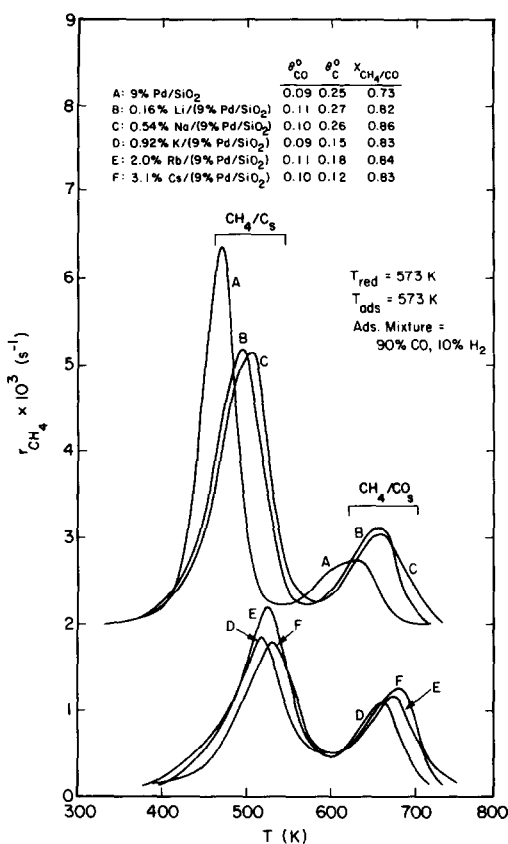


FIG. 10. Effects of the presence of H_2 during CO adsorption on CH_4 formation during TPSR for alkali-promoted Pd/SiO_2 ; adsorption mixture = 90% CO , 10% H_2 ; $T_{red} = 573$ K, $T_{ads} = 573$ K.

CH_4 formation over the catalysts during TPSR following such an adsorption step. Comparison of Fig. 10 with Fig. 8 shows that all six catalysts exhibit a large increase in the peak for the hydrogenation of carbon after the adsorption of CO in the presence of H_2 .

Comparison of Activities for CO Methanation

The dependence of the methanation activity of each catalyst on temperature was determined by raising the catalyst temperature at 1 K/s in a flowing mixture of synthesis gas. In all cases, the maximum conversion was kept below 1%. An Arrhenius plot for CH_4 production, basing the number of

active sites on H_2 - O_2 titration, is given in Fig. 11 following reduction at 573 K. The catalyst activities decrease in the following order: unpromoted $> Li > Na > K > Rb > Cs$. This order did not change throughout the temperature range studied. The activation energies for methanation are given in Fig. 11. The lowest value of E_a is 25.7 kcal/mol, for 9% Pd/SiO_2 . The activation energies for the promoted catalysts range between 26.7 and 28.8 kcal/mol.

The Arrhenius plots of the methanation activities of the catalysts following reduction at 673 K are shown in Fig. 12. The promoted catalysts, in this case, display a higher activity than Pd/SiO_2 for temperatures below 550 K and apparent activation energies in the range of 10 to 12 kcal/mol. The activities at 473 K increase in the order: unpromoted $< K < Na < Li < Cs = Rb$. With increasing reaction temperature, the apparent activation energies increase, finally reaching values equivalent to those reported in Fig. 11. At temperatures above 670 K, the relative activities of all the catalysts also revert to those seen in Fig. 11.

Small quantities of CO_2 were produced by the catalysts at temperatures above 580 K; the rate of CO_2 formation being higher over the promoted samples than over unpromoted Pd/SiO_2 . A small quantity of CH_3OH was formed over the Li- and Na-promoted catalysts, but none could be detected with any of the other catalysts.

DISCUSSION

H_2 - O_2 Titration

Table 1 shows that promotion of Pd/SiO_2 with an alkali metal causes the Pd dispersion determined by H_2 - O_2 titration to increase by 5 to 7%. A similar effect has been observed previously for K-promoted Ru/SiO_2 (29) and K- and Cs-promoted Ru/Al_2O_3 (28). On the other hand, studies of alkali promotion of other Group VIII metals (30, 31) show either no change or a decrease in the dispersion. The data in Table 1 also demonstrate that while the dis-

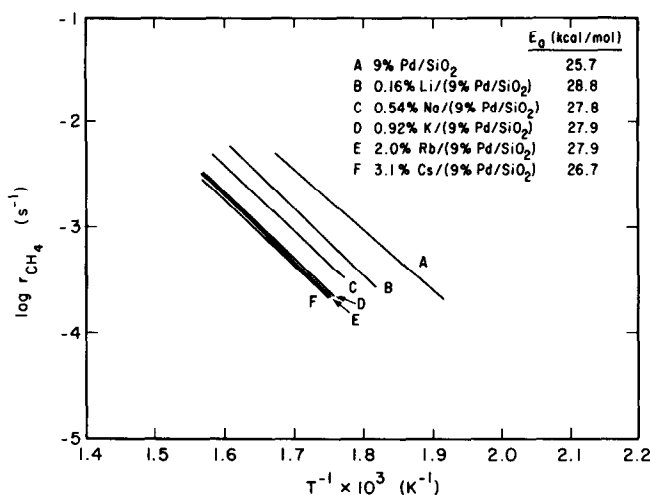


FIG. 11. Comparison of the activities of Pd/SiO₂ and alkali-promoted Pd/SiO₂ for CH₄ production; $P = 1$ atm, H₂/CO = 3/1; $T_{\text{red}} = 573$ K.

persion of Pd/SiO₂ is the same at 573 and 673 K, the dispersion of the promoted catalysts are 1 to 3% lower at the higher temperature. Thus, the promoter may facilitate sintering at high reduction temperatures.

TPR and TPO

The consumption of H₂ during the TPR of Pd/SiO₂ is 1.15×10^{-5} mol (see Table 2) which roughly corresponds to the amount

required to reduce PdO to Pd, 1.36×10^{-5} mol, if it is assumed that during calcination the Pd particles are completely oxidized. Using this assumption, we can then calculate the extent to which the H₂ consumption for the alkali-promoted catalysts exceeds that required to completely reduce the Pd particles to their metallic state. The excess amount of H₂ is given in the second column of Table 2. If this amount of H₂ is attributed

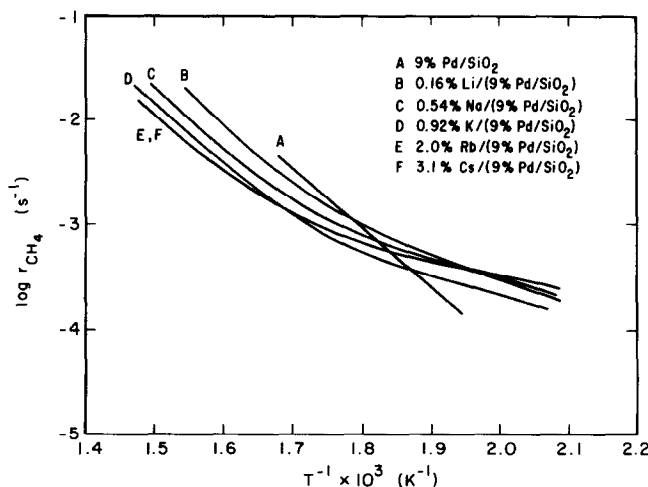


FIG. 12. Comparison of the activities of Pd/SiO₂ and alkali-promoted Pd/SiO₂ for CH₄ production; $P = 1$ atm, H₂/CO = 3/1; $T_{\text{red}} = 673$ K.

to the reduction of the alkali metal oxide, then the moles of oxygen removed per alkali atom can be readily computed, and the result is given in the third column of Table 2. The values of O/M range from 0.55 to as high as 1.61, suggesting that the calcined alkali metal oxide may have a stoichiometry much richer in oxygen than the normal bulk oxide ($O/M = 0.5$). O/M ratios greater than 0.5 are certainly unexpected; however, there is at least one case known in which the conversion of Cs_2O to Cs_2O_2 can occur at the calcination temperature used in this study (32).

H_2 TPD

The spectra for H_2 desorption in Fig. 2 show that the chemisorption of H_2 is not suppressed on the alkali-promoted catalysts following reduction at 573 K. Coverages in excess of a monolayer are observed over the promoted catalysts, in agreement with previous studies of unpromoted Pd/SiO₂ (18) and Pd single crystals (33, 34). Only when the reduction temperature is increased to 673 K is a small suppression of H_2 chemisorption observed. The absence of a large suppression in H_2 chemisorption agrees with the results of Huang and Richardson (31) for Na-promoted Ni/SiO₂-Al₂O₃. These authors observed that for ratios of Na to surface Ni between 0 and 2.35, the number of surface sites measured by H_2 chemisorption agreed with that calculated from magnetization measurements. However, Sun *et al.* (35) showed that D₂ chemisorption is suppressed to 0.5 of a monolayer on Ni(100) promoted with K to a coverage of $\theta_K = 0.14$ ($\theta_K^{sat} = 0.38$). This suggests that the coverage of the Pd crystallites by alkali promoters is quite small for reduction at 573 K, but is greater for reduction at 673 K.

The spectra in Figs. 2 and 3 show that the energetics of H_2 desorption are slightly altered by alkali promotion. For all of the promoted catalysts, the magnitude of the two low-temperature peaks increases rela-

tive to that of the peak at 540–570 K following reduction at 573 K. However, following reduction at 673 K, these low-temperature peaks decrease in magnitude and the spectra are quite similar to that of the original Pd/SiO₂ sample. The results presented here agree well with those for rare earth oxide- and titania-promoted Pd/SiO₂ for which it was also observed that the energetics of H_2 desorption are not significantly different from those for Pd/SiO₂ (1–3).

CO TPD

The saturation coverages of the alkali-promoted catalysts by CO are similar to those for H_2 . Following reduction at 573 K, the coverages are close to a monolayer, and reduction at 673 K results in only a small suppression in chemisorption capacity. The interpretation of these results in the light of single crystal studies is more difficult than in the case of H_2 adsorption since such studies give contradictory results. Kiskinova (13) observed that saturation of Ni(100) with Na, K, and Cs ($\theta_{Na}^{sat} = 0.50$, $\theta_K^{sat} = 0.38$, $\theta_{Cs}^{sat} = 0.20$) suppressed CO chemisorption to 60% of the saturation value for the clean surface. Crowell *et al.* (36) observed that Rh(111), after promotion with K to a coverage of 0.33 ($\theta_K^{sat} = 0.36$), adsorbed 25% of the saturation value of CO for a clean surface. In contrast to these results, studies of K-promoted Pt(111) have shown that the CO uptake is not affected by promotion. Garfunkel and Somorjai (14) found for Pt(111) that a K coverage of $\theta_K = 0.13$ ($\theta_K^{sat} = 0.33$) did not decrease the saturation uptake of CO. Kiskinova *et al.* (37) further observed that, although the sticking coefficient for CO was greatly decreased by alkali promotion, the saturation coverage by CO of a Pt(111) surface containing 0.33 of a monolayer of K did not change. Based on these observations, it is difficult to project what might be the anticipated influence of alkali promoters on CO chemisorption on Pd.

The TPD spectrum for CO desorption

from 9% Pd/SiO₂ is comprised of four peaks centered at 410, 530, 650, and 790 K. By comparing the CO TPD spectra with the infrared observations of Hicks *et al.* (25), Rieck and Bell (3) were able to assign the peaks at 638 and 773 K to CO bridge bonded on Pd(100) and Pd(111) planes, respectively, and the two low-temperature peaks to linearly adsorbed CO. Promotion of Pd/SiO₂ with an alkali results in a significant redistribution of CO adstates. As shown in Fig. 4, the peaks at 638 and 773 K decrease while the low-temperature peaks increase in magnitude following reduction at 573 K. These changes can be attributed to an increase in the proportion of CO desorbing from linear sites relative to bridge sites. It is interesting to note that the redistribution of CO adstates observed upon alkali promotion bears very strong resemblance to the observations of Somanoto and Sachtler (38) for CO adsorption on Pd–Ag alloys. These authors noted that the presence of Ag on Pd surfaces results in an increase in the magnitude of the IR bands for linearly adsorbed CO coupled with a decrease in the bands for bridge adsorbed CO. This change in the distribution of adstates was attributed to an ensemble effect in which surface Ag atoms block bridge sites for CO adsorption without affecting the linear sites. It seems reasonable to propose that a similar interpretation can be given to explain the effects of alkali promotion.

The effects of alkali promotion on the disproportionation of CO to form CO₂ and carbon can be characterized by the temperature at which CO₂ first appears during the TPD of adsorbed CO and the equivalent coverage of CO converted to CO₂, θ_{CO_2} . Of these two measures, the first is considered to be a more reliable indicator of the extent to which the promoter influences CO disproportionation. The reasons why the quantity of CO₂ released may not be a good measure are twofold. First, not all the oxygen released during CO dissociation may be converted to CO₂, since part of it may react strongly with the partially reduced pro-

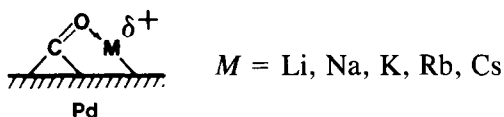
moter. Second, a part of the CO₂ formed may react with the promoter to form a surface carbonate.

Further justification for using the temperature of the onset of CO₂ formation as the measure for the influence of promoters on the dissociation of CO comes from the following observations. Figure 4b shows that after reduction at 573 K, the onset temperature for CO₂ formation is consistently higher for the alkali-promoted samples, relative to unpromoted Pd/SiO₂, indicating a lower activity for CO dissociation. In agreement with this, the table in Fig. 8 indicates that the amount of carbon formed during CO adsorption at 573 K is lower for the promoted samples. When the promoted catalysts are reduced at 673 K, the onset temperature for CO₂ formation decreases to a level below that for unpromoted Pd/SiO₂, leading to the expectation that reduction of the promoted catalysts at 673 K makes them more effective for CO dissociation. The table in Fig. 9 bears out this prediction in that it shows the coverage of carbon on the promoted catalyst, following CO adsorption at 573 K, to be higher than that on the unpromoted catalyst. The net conclusion then is that the influence of alkali promoters on the dissociation of CO is a function of the temperature at which the catalyst has been reduced: reduction at 573 K results in lower CO dissociation activity for the promoted catalysts, relative to unpromoted Pd/SiO₂, but reduction at 673 K reverses this relationship.

The lower effectiveness for CO dissociation on alkali-promoted Pd/SiO₂ reduced at 573 K, relative to unpromoted Pd/SiO₂, may be due to the influence of the promoter in shifting the adsorption of CO toward linear states. Recent calculations by Baetzold (39) have shown that the activation energy for CO dissociation from bridge sites is considerably lower than that for dissociation from linear sites on fcc(111) surfaces. Consistent with this, Rieck and Bell (18) have noted that the increase in CO dissociation activity with decreasing Pd dispersion for

Pd/SiO₂ can be ascribed to the higher proportion of bridge sites on planar surfaces on the larger metal particles.

The higher effectiveness for CO dissociation on alkali-promoted Pd/SiO₂ reduced at 673 K, relative to unpromoted Pd/SiO₂, may be due to two effects. The first is the restabilization of CO adsorption in bridge sites. This is the effect predicted by Anderson and Awad (40) for Pd promoted with alkali metal atoms. The second is an interaction of the oxygen end of an adsorbed CO molecule with an atom of alkali metal present on the Pd surface as shown below.



The consequence of such an interaction would be to weaken the C—O bond, thereby facilitating CO dissociation. Weakening of the C—O bond by enhanced back-donation of *d*-electrons from the metal to the 2 π^* orbital of CO, such as has been reported for alkali promotion of Rh(111) (36), Ni(100) (13, 15), Fe(100) (41), and Fe(110) (42) surfaces, is not expected. Rogozik *et al.* (43) have established that the 2 π^* orbital of CO adsorbed on a Pd(100) surface lies too far above the Fermi level to permit back-donation from the *d*-orbitals of the metal. As a consequence, even if the density of states at the Fermi level were increased due to charge transfer from adsorbed alkali to the metal, it is unlikely that the extent of back-donation to the 2 π^* orbital of CO would be increased.

TPSR of Adsorbed CO

Studies of Pd/SiO₂, TiO₂-promoted Pd/SiO₂, and rare earth oxide-promoted Pd/SiO₂ (1–3) have shown that the carbon formed by the predissociation of CO is much more easily hydrogenated than molecular CO, indicating that CO dissociation is the rate-limiting step in the formation of methane. A similar conclusion can be drawn for the alkali-promoted catalysts,

since, as shown in Figs. 8–10, the reactivity of surface carbon is always greater than that of molecular CO. The differences in the rates of methanation of adsorbed CO over unpromoted Pd/SiO₂ and Pd/SiO₂ promoted with different alkali metals observed in Figs. 6a, 8, and 10 must, therefore, be due to the influence of the promoter on the rate of CO dissociation. Consistent with this interpretation, we see from Fig. 4b that the onset temperature for the appearance of CO₂ (which as noted previously is a good index of catalyst activity for CO dissociation) increases in the order: unpromoted < Li < Na < K < Rb < Cs. Thus, the high activity of unpromoted Pd/SiO₂ can be ascribed to the greater ease with which CO dissociates over this catalyst.

Following the logic presented above, one might expect the promoted catalysts reduced at 673 K to be more active for the methanation of adsorbed CO, since as seen in Fig. 5b, the onset temperature for CO₂ formation is lower than that for unpromoted Pd/SiO₂. Figure 7a shows this not to be the case. The most likely reason for the apparent inconsistency is that the water formed during the early stages of CO methanation rapidly reoxidizes the promoter, thereby spoiling its effectiveness for further CO dissociation. A similar argument can be advanced to explain the ordering of the peaks designated CH₄/CO_s in Fig. 9.

In addition to affecting the dissociation of CO, the decoration of Pd with alkali metal species alters the reactivity of adsorbed carbon. Figure 8 shows that the peak temperature for hydrogenation of adsorbed carbon increases with alkali promotion, with a maximum upscale shift of 67 K for Cs-promoted Pd/SiO₂. Since the kinetics of carbon hydrogenation are first-order in carbon coverage (44, 45) this shift indicates that the carbon is less reactive. A similar result, although much smaller in magnitude, was observed for titania- and rare earth oxide-promoted Pd/SiO₂ (1, 2). The reasons for the lower reactivity of the adsorbed carbon on the promoted samples is not clear. How-

ever, if an electronic effect is responsible, it might be expected that the reactivity of the carbon should vary monotonically with the increasing electropositive nature of the alkali metals. As shown in Fig. 8, this is indeed the case. The least reactive carbon is that deposited on the catalyst with the most electropositive promoter, Cs.

Evidence for the lower reactivity of adsorbed carbon in the presence of alkali promoters has been reported previously for Fe (46), Ni (15), and Ru (29) catalysts. For these catalysts, it was observed that under reaction conditions, larger deposits of carbon accumulated on the surface of the catalysts in the presence of alkali promoters. In the case of K-promoted Ni(100) (15), the amount of surface carbon at steady state increased by up to a factor of 3 relative to an unpromoted Ni(100) surface. This was attributed to a combination of an increase in dissociation activity and a decrease in carbon reactivity. A possible explanation for the lower reactivity of carbon on alkali-promoted catalysts, suggested by McLaughlin McClory and Gonzalez for Ru catalysts (29), is that the alkali metal promoter inhibits carbon hydrogenation by site blockage. However, since the chemisorption of CO and H₂ were not significantly suppressed by the promoters in the present study, it is unlikely that this is the case for Pd.

The activation energies shown in Fig. 8 for methanation over the alkali-promoted catalysts reduced at 573 K range between 26.7 and 28.8 kcal/mol, while that for Pd/SiO₂ is 25.7 kcal/mol. The higher activation energy over the promoted catalysts indicate that the energetics for the reaction are less favorable. This is consistent with the lower dissociation activity and the lower reactivity of the adsorbed carbon on these samples. The methanation activity decreases with increasing electropositive nature of the alkali promoter, which is the same trend as seen for the reactivity of the surface carbon. The lower methanation activity of these catalysts is in agreement with pre-

vious studies of alkali-promoted Pd (5, 7), Rh (47), Ni (15, 48), Fe (46, 49), and Ru (29) catalysts. Only for Ni supported on SiO₂-Al₂O₃ (31, 48) has an increase in activity been reported upon promotion with an alkali.

Following reduction at 673 K, the promoted catalysts display a higher methanation activity at low temperatures (<550 K) than unpromoted Pd/SiO₂. As was mentioned previously, this may be attributed to a more extensive reduction of the alkali promoter than can be achieved at 573 K. Figure 9 shows that reducing the promoted catalysts at 673 K results in a higher activity for CO dissociation relative to Pd/SiO₂. Thus, the oxygen-deficient alkali metal oxide species assist the dissociation of CO, along with increasing the low-temperature activity of these catalysts for CO hydrogenation. The more favorable reaction energetics are reflected by the small initial slopes of the Arrhenius plots shown in Fig. 12 for the promoted samples. The curvature in the Arrhenius plots for the promoted samples shown in Fig. 12 can be attributed to reoxidation of the promoter caused by water produced during CO hydrogenation. The net result of this effect is that at the highest temperatures used in this study, the alkali oxide becomes an inhibitor and the order of catalyst activities reverts to that seen in Fig. 11. Consistent with the proposed interpretation, it was observed that upon reduction of the reaction temperature, following reaction at high temperatures, each of the catalysts produced a straight Arrhenius line with a slope similar to that seen in Fig. 11. Thus, it is apparent that the state of the promoted Pd/SiO₂ catalysts achieved by reduction at 673 K is not stable under reaction conditions where substantial amounts of water are present.

CONCLUSIONS

The effects of alkali promotion of Pd/SiO₂ on the adsorption and reaction of H₂ and CO are a strong function of the temper-

ature at which the catalyst is reduced. Following reduction at 573 K, the distribution of H_2 adstates is essentially the same for the promoted and unpromoted catalysts. By contrast, the CO adstate distribution shifts towards a higher proportion of linearly adsorbed species and a lower proportion of bridge adsorbed species for the promoted Pd/SiO₂, relative to unpromoted Pd/SiO₂. This pattern is attributed to ensemble effects in which bridge sites are blocked by the promoter. The dissociation of CO occurs less readily over the promoted catalysts reduced at 573 K due to the lower activity of linear sites relative to bridge sites for CO dissociation. Reduction of the promoted catalysts at 673 K causes little change in the distribution of H_2 adstates, but restores the distribution of CO adstates to one which is similar to that for unpromoted Pd/SiO₂. Reduction at 673 K increases the CO dissociation activity of the promoted samples relative to unpromoted Pd/SiO₂ due to the participation of reduced alkali species in the rupture of the C—O bond. This enhanced activity is easily reversed by the oxygen formed by the dissociation of CO or by exposure of the catalyst to water.

The formation of methane by the reduction of carbon formed by the dissociation of CO proceeds much more rapidly than by the reduction of adsorbed CO, indicating that CO dissociation is the rate-limiting step in the methanation of CO over Pd. The steady-state activity of the catalysts studied decreases in the order: unpromoted > Li > Na > K > Rb > Cs, paralleling the activity for CO dissociation. It is also observed that alkali promotion decreases the reactivity of adsorbed carbon with H_2 , the effect increasing with the electropositive character of the alkali.

ACKNOWLEDGMENT

This work was supported by the Division of Chemical Sciences, Office of Basic Energy Sciences, United States Department of Energy, under Contract DE-AC03-76SF00098.

REFERENCES

1. Rieck, J. S., and Bell, A. T., *J. Catal.* **96**, 88 (1985).
2. Rieck, J. S., and Bell, A. T., *J. Catal.*, in press.
3. Rieck, J. S., and Bell, A. T., *J. Catal.*, in press.
4. Driessen, J. M., Poels, E. K., Hindermann, J. P., and Ponec, V., *J. Catal.* **82**, 26 (1983).
5. Kikuzono, Y., Kagami, S., Naito, S., Onishi, T., and Tamaru, K., *Faraday Discuss. Chem. Soc.* **72**, 135 (1982).
6. Kelly, K. P., Tatsumi, T., Uematsu, T., and Lunsford, J. H., *J. Catal.*, in press.
7. Yoshioka, H., Naito, S., and Tamaru, K., *Chem. Lett.*, 981 (1983).
8. Deligianni, H., Mieville, R. L., and Peri, J. B., in "Proceedings, 8th International Congress on Catalysis, Berlin," Vol. V. p. 243, 1984.
9. Bracey, J. D., and Burch, R., *J. Catal.* **86**, 384 (1984).
10. Anderson, J. B. F., Bracey, J. D., Burch, R., and Flambard, A. R., in "Proceedings, 8th International Congress on Catalysis, Berlin," Vol. V. p. 111. 1984.
11. Kunimori, K., Abe, H., Yamaguchi, E., Matsui, S., and Uchijima, T., in "Proceedings, 8th International Congress on Catalysis, Berlin," Vol. V. p. 251. 1984.
12. Connell, G., and Dumesic, J. A., *J. Catal.* **92**, 17 (1985).
13. Kiskinova, M. P., *Surf. Sci.* **111**, 584 (1981).
14. Garfunkel, E. L., and Somorjai, G. A., *Surf. Sci.* **115**, 441 (1982).
15. Campbell, C. T., and Goodman, D. W., *Surf. Sci.* **123**, 413 (1982).
16. Sachtler, W. M. H., in "Proceedings, 8th International Congress on Catalysis, Berlin," Vol. V. p. 151. 1984.
17. Sachtler, W. M. H., Shriver, D. F., Hollenberg, W. B., and Long, A. F., *J. Catal.* **92**, 429 (1985).
18. Rieck, J. S., and Bell, A. T., *J. Catal.*, in press.
19. Ichikawa, S., Poppa, H., and Boudart, M., *J. Catal.* **91**, 1 (1985).
20. Hicks, R. F., and Bell, A. T., *J. Catal.* **90**, 205 (1984).
21. Doering, D. L., Poppa, H., and Dickinson, J. T., *J. Catal.* **73**, 104 (1982).
22. Low, G., and Bell, A. T., *J. Catal.* **57**, 397 (1979).
23. Uchida, M., and Bell, A. T., *J. Catal.* **60**, 204 (1979).
24. Chin, A. A., and Bell, A. T., *J. Phys. Chem.* **87**, 3700 (1983).
25. Hicks, R. F., Yen, Q.-J., and Bell, A. T., *J. Catal.* **89**, 498 (1984).
26. Fleisch, T. H., Hicks, R. F., and Bell, A. T., *J. Catal.* **87**, 398 (1984).
27. Rieck, J. S., and Bell, A. T., *J. Catal.* **85**, 143 (1984).

28. Aika, K., Shimazaki, K., Hattori, Y., Ohya, A., Ohshima, S., Shiota, K., and Ozaki, A., *J. Catal.* **92**, 296 (1985).
29. McLaughlin McClory, M., and Gonzalez, R. D., *J. Catal.* **89**, 392 (1984).
30. Dry, M. E., and Oosterhuizen, G. J., *J. Catal.* **11**, 18 (1968).
31. Huang, C. P., and Richardson, J. T., *J. Catal.* **51**, 1 (1978).
32. Frost, D. C., Ishitani, A., and McDowell, C. A., *Mol. Phys.* **24**, 861 (1972).
33. Behm, R. J., Christmann, K., and Ertl, G., *Surf. Sci.* **99**, 320 (1980).
34. Cattania, M. G., Penka, V., Behm, R. J., Christmann, K., and Ertl, G., *Surf. Sci.* **126**, 382 (1983).
35. Sun, Y.-M., Luftman, H. S., and White, J. M., *Surf. Sci.* **139**, 379 (1984).
36. Crowell, J. E., Garfunkel, E. L., and Somorjai, G. A., *Surf. Sci.* **121**, 303 (1982).
37. Kiskinova, M., Pirug, G., and Bonzel, H. P., *Surf. Sci.* **133**, 321 (1983).
38. Somanoto, Y., and Sachtler, W. M. H., *J. Catal.* **32**, 315 (1974).
39. Baetzold, R. C., *J. Phys. Chem.* **82**, 15 (1985).
40. Anderson, A. B., and Awad, M. K., Chemistry Department, Case Western Reserve University, Cleveland, Ohio, private communication.
41. Benzinger, J., and Madix, R. J., *Surf. Sci.* **94**, 119 (1980).
42. Broden, G., Gafner, G., and Bonzel, H. P., *Surf. Sci.* **84**, 295 (1979).
43. Rogozik, J., Kuppers, J., and Dose, V., *Surf. Sci.* **148**, L653 (1984).
44. Winslow, P., and Bell, A. T., *J. Catal.* **86**, 158 (1984).
45. Ozdogan, S. Z., Gochis, P. D., and Falconer, J. L., *J. Catal.* **83**, 257 (1983).
46. Bonzel, H. P., and Krebs, H. J., *Surf. Sci.* **109**, L527 (1981).
47. Chuang, S. C., Goodwin, J. G., and Wender, I., *J. Catal.* **92**, 416 (1985).
48. Chai, G.-Y., and Falconer, J. L., *J. Catal.* **93**, 152 (1985).
49. Arakawa, H., and Bell, A. T., *Ind. Eng. Chem. Proc. Des. Dev.* **22**, 97 (1983).